a function of f_n. It is seen that the statistics of this system are complex, but intuitively an inequality is clear: for a given molecular weight and cross-link number $g_{random} \leq g_{quasi\text{-}random} \leq g_{ring\ weighted}$.

Finally, the fundamental difference between these types of intramolecular cross-linking is exemplified by the natural variables for each process. The ring-weighted contraction factor is a universal function of the cross-link density, the random contraction factor is a universal function of the cross-link number, and the quasi-random g is a complex function of the cross-link number and the molecular weight. With the effects of excluded volume added, it should be mentioned that contraction in dimensions always depends on both the molecular weight and the cross-link number, regardless of the type of cross-linking employed.

Acknowledgment. We are indebted to J. M. Schurr for generously providing the use of his photon correlation spectroscopy laboratory and for his many helpful suggestions concerning these measurements.

Registry No. Polystyrene, 9003-53-6; *p*-bis(chloromethyl)-benzene, 623-25-6.

References and Notes

(1) B. H. Zimm and W. H. Stockmayer, *J. Chem. Phys.*, **17**, 1301 (1949).
(2) V. W. Kuhn and G. Balmer, *J. Polym. Sci.*, **57**, 311 (1962).
(3) P. Longi, F. Greco, and U. Rossi, *Makromol. Chem.*, **116**, 113 (1968).
(4) P. Longi, F. Greco, and U. Rossi, *Makromol. Chem.*, **129**, 157 (1969).
(5) V. W. Kuhn and H. Majer, *Makromol. Chem.*, **18/19**, 239 (1955).
(6) G. Allen, J. Burgess, S. F. Edwards, and D. J. Walsh, *Proc. R. Soc. London, Ser. A*, **334**, 453 (1973).
(7) G. Allen, J. Burgess, S. F. Edwards, and D. J. Walsh, *Proc. R. Soc. London, Ser. A*, **334**, 465 (1973).
(8) G. Allen, J. Burgess, S. F. Edwards, and D. J. Walsh, *Proc. R. Soc. London, Ser. A*, **334**, 477 (1973).
(9) N. B. Vargaftik, "Tables on the Thermophysical Properties of Liquids and Gases", Wiley, New York, 1975.
(10) W. Bushuk and H. Benoit, *Can. J. Chem.*, **36**, 1616 (1958).
(11) N. Grassie and J. Gilks, *J. Polym. Sci., Polym. Chem. Ed.*, 11, 1531 (1973).
(12) W. H. Stockmayer and M. Fixman, *J. Polym. Sci., Part C*, **1**, 137 (1963).
(13) M. Kurata and H. Yamakawa, *J. Chem. Phys.*, **29**, 311 (1958).
(14) H. Yamakawa and M. Kurata, *J. Phys. Soc. Jpn.*, **13**, 94 (1958).
(15) H. Yamakawa and G. Tanaka, *J. Chem. Phys.*, **55**, 3188 (1971).
(16) J. Shimada and H. Yamakawa, *J. Polym. Sci., Polym. Phys. Ed.*, **16**, 1927 (1978).
(17) G. Tanaka, *Macromolecules*, **15**, 1028 (1982).
(18) P. J. Flory and T. Fox, *J. Am. Chem. Soc.*, **73**, 1904 (1951).
(19) H. Yamakawa, "Modern Theory of Polymer Solutions", Harper and Row, New York, 1971.
(20) P. J. Flory, "Principles of Polymer Chemistry", Cornell University Press, Ithaca, NY, 1953.
(21) H. Inagaki, H. Suzuki, M. Fujii, and T. Matsui, *J. Phys. Chem.*, **70**, 1718 (1966).
(22) T. A. Orofino and A. Ciferri, *J. Phys. Chem.*, **68**, 3136 (1964).
(23) B. H. Zimm, *J. Chem. Phys.*, **14**, 164 (1946).
(24) A. C. Albrecht, *J. Chem. Phys.*, **27**, 1002 (1957).
(25) E. F. Casassa, *J. Chem. Phys.*, **37**, 2176 (1962).
(26) E. F. Casassa, *J. Chem. Phys.*, **41**, 3213 (1964).
(27) E. F. Casassa, *J. Polym. Sci., Part A*, **3**, 605 (1965).
(28) S. Saeki, N. Kuwahara, S. Konno, and M. Kanedo, *Macromolecules*, **6**, 589 (1973).
(29) A. Liu, E. F. Casassa, and G. C. Berry, private communication.
(30) L. Leger, H. Hervet, H. Deshamps, and G. Guillot, private communication.
(31) H. Yamakawa, *J. Chem. Phys.*, **36**, 2995 (1962).
(32) S. Imai, *J. Chem. Phys.*, **50**, 2116 (1969).
(33) M. J. Pritchard and D. Caroline, *Macromolecules*, **13**, 957 (1980).
(34) G. Jones and D. Caroline, *Chem. Phys.*, **37**, 187 (1979).
(35) W. H. Stockmayer and A. C. Albrecht, *J. Polym. Sci.*, **32**, 215 (1958).
(36) J. G. Kirkwood, *Recl. Trav. Chim. Pays-Bas*, **68**, 649 (1949).
(37) M. Kurata and M. Fukatsu, *J. Chem. Phys.*, **41**, 2934 (1964).
(38) W. H. Stockmayer and M. Fixman, *Ann. N.Y. Acad. Sci.*, **57**, 334 (1953).
(39) O. B. Ptitsyn, *Zh. Tekh. Fiz.*, **29**, 75 (1959).
(40) M. A. Winnik, A. E. C. Redpath, and G. L. Petrasinunas, *Proc. IUPAC MACRO 82*, **28**, 553 (1982).

Scaling Picture for Polymer Melt Rheology: A Critique of the Curtiss–Bird Model

Douglas A. Bernard and Jaan Noolandi*

Xerox Research Centre of Canada, 2480 Dunwin Drive, Mississauga, Ontario, L5L 1J9 Canada. *Received April 5, 1982*

ABSTRACT: The reptation concept of de Gennes has recently been combined with kinetic theory and incorporated into a new model of polymer melt rheology by Curtiss and Bird (CB). We discuss the structure of this model by regarding it as an extension of dilute solution theory to concentrated systems. We examine the linear viscoelastic predictions of the CB model by carrying out detailed calculations of the storage and loss modulus curves and comparing them with experimental data for polystyrene. We discuss in depth the modified form of Stokes' law and introduce a scaling picture of the CB model chain. Using this scaling picture, we argue that the only value of the link tension coefficient ϵ consistent with both the internal subchain structure and the bead–rod configuration of the model chain is $\epsilon = 0$. Our interpretation of kinetic theory in concentrated polymer systems strongly suggests applying the reptational constraint to a scaling picture with Rouse-like chains.

1. Introduction

Viscoelastic properties of high-polymer melts have acquired renewed interest and a very interesting perspective in the recent development by Curtiss and Bird[1] (CB) and by Doi and Edwards[2] (DE) of microscopic theories of rheology which incorporate the reptation idea of de Gennes.[3] Prior to the development of these models, concentrated polymeric systems have resisted theoretical analysis due to the difficult problem of entanglement effects.

The reptation model provides a key to the study of concentrated polymers since it describes these effects in a simple and fundamental way. In essence it uses Edwards'

0024-9297/83/2216-1358$01.50/0

earlier concept[4] that entanglement constraints act effectively as an open-ended confining tube that surrounds any given macromolecular chain along its average contour, and then asserts that the chain diffuses in a one-dimensional manner, although it is free to seek new three-dimensional configurations.

Using this picture, de Gennes[3,5] analyzed the dynamics of reptation for the special case of a single chain reptating inside a three-dimensional network of fixed obstacles. However, the real polymer melt consists of many interacting and mobile chains, and thus it is not surprising that the reptation model in its original form is questioned by comparison with experimental data. For linear homopolymers the zero-shear viscosity, η, appears to increase with molecular weight according to the celebrated[6] empirical power law $\eta \propto M^{3.4}$, in disagreement with the exponent of 3 predicted by de Gennes' discussion. In addition to mechanisms of tube constraint relaxation,[7,8] alternate explantations for this discrepancy have been advanced.[9,10] Polydispersity effects have also been proposed,[11,12] but after careful analysis we have found[13] they do not resolve the discrepancy in the form suggested.

The simplicity of the reptation concept and the notion of its fundamental correctness strongly motivate further study and development, especially through its inclusion in detailed molecular theories of rheology for entangled polymeric systems. At present, Doi and Edwards[2] have constructed a stochastic model of reptating chains, while Curtiss and Bird[1] (CB) have applied the phase-space kinetic theory[14,15] to this problem. Unfortunately, both theories remain mean field theories with respect to entanglement effects, and neither considers modifications to the original reptation picture arising from motions of the constraint-producing chains. However, each model directly incorporates the effects of reptation in the detailed prediction of rheological functions.

This paper focuses on the Curtiss–Bird model. In section 2 we discuss its structure and physical assumptions. By viewing the CB model as an extension of the concepts of dilute solution theory to concentrated systems, we give a critical examination of the modified Stokes' law employed by Curtiss and Bird and comment on the link tension coefficient and the chain constraint exponent. Our analysis is guided by our interpretation of the CB model chain as a thinned-out version of the real chain. In section 3 we discuss rheological properties and numerically calculate the theoretical storage and loss modulus curves. The CB formulas for the plateau modulus and the characteristic relaxation time are rewritten in terms of the intrinsic properties of the real chain and the scale factor used in reducing this chain. Subsequently, the CB model is compared with existing rheological data on melt polystyrene in section 4, and the values of the parameters determined by this data are presented and discussed.

2. Physical Assumptions of the Curtiss–Bird Model

The starting point for the Curtiss–Bird model is the phase–space kinetic theory for macromolecular liquids.[14,15] This theory provides a rigorous derivation of the fluid equations of motion and yields explicit expressions for hydrodynamic quantities in terms of molecular interactions and distribution functions. The CB model applies the phase–space kinetic theory to the special case in which the polymer molecule is idealized as a freely jointed bead–rod chain with a *fixed bead separation* or rod length a.

In view of the mathematical complexity underlying the CB model, it is very instructive to compare it with the more familiar model of Rouse.[16] This is possible because the phase–space kinetic theory contains the Rouse model as a special case and because both models utilize similar concepts. In particular, each model works with a chain of beads and operates in a single-chain configuration space of internal bead coordinates Q. A diffusion equation describes the time evolution of the configuration space distribution function $\psi(Q,t)$ in the presence of a specified flow field $\mathbf{v}(\mathbf{r},t)$. Since the Rouse model describes isolated chains immersed in a solvent, the velocity field is provided by the solvent molecules. In the CB model it is provided by the bulk flow of background chains. The diffusion equation is obtained by using the continuity equation, which has the schematic form

$$\partial_t\psi + \partial_Q(\langle\dot{Q}\rangle\psi) = 0 \tag{2.1}$$

and eliminating $\langle\dot{Q}\rangle$, the configuration space flow, by means of a force equation that balances Brownian forces with intermolecular forces, neglecting transient acceleration terms:

$$F_{\text{Brownian}} + F_{\text{intermolecular}} = 0 \tag{2.2}$$

Apart from the connection of adjacent beads and the assumption of ideal chains, intramolecular forces are neglected in each model. The Brownian force expresses the tendency of the internal coordinates to flow in the direction where the molecular configuration is the most probable one and involves spatial derivatives of the configuration space distribution function. The intermolecular force contains $\langle\dot{Q}\rangle$ because it is approximated by Stokes' law, which is a mean field treatment of the interaction of the average chain with its environment. This represents the viscous drag between the molecule and the background flow, provided by the solvent in the Rouse case and by the neighboring chains in the CB model. In both models, this force is directed at the beads of the chain.

(a) Stokes' Law Assumption. Although both the Rouse and the CB models employ Stokes' law, there are important modifications in the treatment of intermolecular forces. One feature is a modified Stokes' law, implying that the drag force on an individual bead no longer has the standard isotropic form employed in the Rouse model, namely

$$(\mathbf{F}_{i,\text{Stokes}})_{\text{Rouse}} = -\zeta[\langle\dot{\mathbf{r}}_i\rangle - \mathbf{v}(\mathbf{r}_i,t)] \tag{2.3}$$

where $\mathbf{F}_{i,\text{Stokes}}$ is the Stokes' drag experienced by the ith bead, ζ is a phenomenological scalar friction coefficient, $\mathbf{r}_i$ is the bead position, and $\langle\dot{\mathbf{r}}_i\rangle$ is its average velocity. Instead, the CB form has an additional contribution determined by the positions and motions of the other beads in the chain. This is more clearly seen by working with $\Delta\mathbf{F}_{\text{Stokes}}$, defined as the difference in the frictional forces on a pair of adjacent beads, connected by the vector $\mathbf{x}$ and located in a flow field of uniform velocity gradient κ. In the Rouse model, eq 2.3 yields

$$(\Delta\mathbf{F}_{\text{Stokes}})_{\text{Rouse}} = -\zeta[\langle\dot{\mathbf{x}}\rangle - \kappa\cdot\mathbf{x}] \tag{2.4}$$

Curtiss and Bird modify this by using a nonisotropic friction coefficient depending on the orientation of the rod that connects the pair of beads. It is given in tensor form by

$$\zeta(\mathbf{u}) = \zeta[\delta - (1-\epsilon)\mathbf{uu}] \tag{2.5}$$

where δ is the unit tensor, $\mathbf{u} = \mathbf{x}/a$ is the unit vector describing the link orientation, and ϵ is the link tension coefficient, to be discussed below. The relative Stokes' force is then defined by

$$(\Delta\mathbf{F}_{\text{Stokes}})_{\text{CB}} = -N^{\beta}\zeta(\mathbf{u})\cdot[\langle\dot{\mathbf{u}}\rangle - \kappa\cdot\mathbf{u}]a \tag{2.6}$$

Note that in the CB model the separation between beads

is fixed, so the average relative bead velocity reduces to $\langle \dot{\mathbf{x}} \rangle = a\langle \dot{\mathbf{u}} \rangle$.

The additional factor N^β appearing in eq 2.6 represents a postulated enhancement of the scalar part of the friction coefficient per bead for long chains due to the presence of an entanglement newwork, the chain constraint exponent β being positive but unknown. We view this factor as an attempt to account in the context of the mean field approximation for many-body effects occurring when a bead rubs against a medium whose components are strongly interacting. In polymer melts, the medium consists of monomers belonging to flexible chains forming an entanglement network, and the effective interaction should depend on the degree of entanglement, which increases with N. Since the beads must drag part of the network, rather than just its individual components, the phenomenon is roughly analogous to the Mössbauer effect.[17] This contrasts completely with the Rouse model, where the macromolecules are immersed in a medium consisting of low molecular weight solvent.

It is also important to understand the parameter ϵ contained in the CB form of Stokes' law because it has a significant effect on rheological predictions, as we show in section 3 (see Figure 2). To discuss ϵ, we assert that the N-bead model chain employed in the CB model should be regarded as a thinned-out version of the real chain, in which degrees of freedom are hidden between each adjacent pair of beads in the form of a submolecule or blob consisting of real monomers, q in number. This scheme is supported for the CB model by our comparison with linear viscoelastic data, where in the specific case of polystyrene we fit the plateau storage modulus, which is independent of ϵ, and find the blob size to be $q \simeq 36$ monomers per subchain (see section 4).

In addition, by analyzing the effects of subchain structure in the CB model, we find that the only value of ϵ consistent with the bead–rod configuration of the model chain is $\epsilon = 0$. The modified form of Stokes' law implies that the net axial component of the relative Stokes' drag for adjacent beads is proportional to ϵ:

$$\mathbf{u}\cdot(\Delta\mathbf{F}_{\text{Stokes}})_{\text{CB}} \propto \epsilon \tag{2.7}$$

Here, $\mathbf{u} = \mathbf{x}/a$ is the unit vector describing the link orientation. Thus ϵ is the link tension coefficient: when $\epsilon = 0$, the forces of constraint vanish. But for nonzero ϵ, nonvanishing and *variable* constraint forces are needed to maintain the fixed interbead separation. However, this is incompatible with the available internal force provided by Brownian motion within the subchain, since this force must be *fixed* given fixed subchain size and subchain equilibrium. Moreover, the equilibrium properties of Rouse-like subchains imply that the available link tension vanishes.

However, $\epsilon = 0$ implies a nonisotropic form of Stokes' law since anisotropy in the CB friction coefficient is determined by the quantity $1-\epsilon$. The tensor friction coefficient of eq 2.5 modifies the relative drag force on the end beads of each rod from the form used in the Rouse model (see eq 2.4) by adding an extra component along the axis of the rod, giving

$$(\Delta\mathbf{F}_{\text{Stokes}})_{\text{CB}} = N^\beta(\Delta\mathbf{F}_{\text{Stokes}})_{\text{Rouse}} + (\epsilon - 1)\mathbf{u}(N^\beta\zeta a\mathbf{u}\cdot\boldsymbol{\kappa}\cdot\mathbf{u}) \tag{2.8}$$

In contrast to the chain constraint exponent β, we find this difficult to justify. It is not clear how the second term in eq 2.8 accounts for entanglement or tube constraint effects since it vanishes when the velocity gradient κ is zero.

(b) Scaling Picture. A scaling approach is useful for a discussion of the CB model because it implies that the parameters N, m, a, and ζ characterizing the reduced chain scale in proportion to those of the real chain. Since each submolecule or blob consists of q real monomers, the molecular weight of each bead must be

$$m = qm_u \tag{2.9}$$

where m_u is the monomer molecular weight. Similarly, the number N of beads or blobs is related to the number N_u of monomers in the real chain by

$$N = N_u/q \tag{2.10}$$

Additionally, chains in the melt state are ideal,[5,18] so for sufficiently large q the conformational statistics of each submolecule will be Gaussian. Consequently, the interbead separation, taken to be the root-mean-square size of a blob in equilibrium, is

$$a = a_u q^{1/2} \tag{2.11}$$

where a_u is the effective size of a monomer in the melt. Since the frictional properties of the beads are ultimately determined by those of the blobs they simulate, it is also reasonable to assume that the net frictional drag on a bead is obtained by adding the contribution of each consituent monomer. This is expressed by

$$\zeta = q\zeta_u \tag{2.12}$$

where ζ_u is the friction coefficient of each monomer in the melt. In each of these equations the sole parameter determining the reduction of the real chain is the number of monomers per submolecule, q.

As an example of the usefulness of the scaling picture, we estimate the characteristic blob relaxation time τ_{blob}, regarding the blob as a miniature Rouse chain of mass m and using the lifetime of the slowest Rouse mode. The Rouse expression for the relaxation time of the nth mode in a chain consisting of N subchains is[16]

$$\tau_n \simeq \zeta a^2N^2/6\pi^2kTn^2 \tag{2.13}$$

If we define the q-independent or intrinsic measure of the friction coefficient as

$$\gamma = \zeta a^2/m^2 = \zeta_u a_u{}^2/m_u{}^2 \tag{2.14}$$

we can cast eq 2.13 in a form that is manifestly independent of the choice of subchain size. Using $mN = m_uN_u = M$, where M is the molecular weight of the overall chain, eq 2.14 becomes

$$\tau_n \simeq \gamma M^2/6\pi^2kTn^2 \tag{2.15}$$

This shows explicitly that the Rouse model has the desirable property that the longest relaxation time τ_1 is independent of the subchain size and depends only on the intrinsic properties of the real chain. We finally obtain τ_{blob} by replacing M by the blob mass m in the expression for τ_1:

$$\tau_{\text{blob}} \simeq \gamma m^2/6\pi^2kT \tag{2.16}$$

from which we can show that at low frequencies the CB model is consistent with local equilibrium of subchains.

3. Linear Viscoelasticity in the Curtiss–Bird Model

We now discuss the linear viscoelastic behavior predicted for polymer melts by the CB model. This is contained in the lowest order rheological equation of state, which is the linearized version of the relation derived between stress, τ, and strain rate $\dot{\gamma}$. It expresses the time-dependent

Table I
Microscopic Expressions for the Plateau Modulus G^0_N and the Characteristic Relaxation Time τ in the Doi-Edwards[2] and Curtiss-Bird[1] Models[a]

	Curtiss-Bird	Doi-Edwards
G^0_N	$(1/5)\nu NkT$	$(4/5)\nu NkT$
	$(1/5)(\rho RT/m_u)q^{-1}$	$(4/5)(\rho RT/m_u)q^{-1}$
τ	$\frac{N^{3+\beta}\zeta a^2}{2\pi^2 kT}$	$\frac{N^3\zeta a^2}{\pi^2 kT}$
	$\frac{M^{3+\beta}(qm_u)^{-(1+\beta)}\gamma}{2\pi^2 kT}$	$\frac{M^3(qm_u)^{-1}\gamma}{\pi^2 kT}$

[a] The original form is given, followed by the rewritten version based on the scaling picture of the model chain, with q = subchain size and γ = intrinsic friction coefficient (see section 2).

memory effects present in viscoelastic systems and takes the well-known general form[15]

$$\tau(t) = -\int_{-\infty}^{t} G(t-s)\dot{\gamma}(s)\,ds \tag{3.1}$$

The response function $G(t)$ contains the linear viscoelastic behavior and is called the relaxation modulus.

In discussing the form of $G(t)$ predicted by the CB model, there are two independent considerations: the shape and the scaling. This follows because the structure of the model relaxation spectrum is universal, allowing $G(t)$ to be written in the dimensionless form

$$G(t) = G^0_N g_R(\tilde{t}) \tag{3.2}$$

The variable $\tilde{t} \equiv t/\tau$ represents time in units of a characteristic relaxation time τ. The scale of the modulus is set by G^0_N, identified as the plateau storage modulus. The shape is contained in the reduced modulus $g_R(\tilde{t})$, defined by eq A.1 in Appendix A. We first consider the scaling variables G^0_N and τ.

Our earlier claim that the N-bead model chain employed by Curtiss and Bird should be interpreted as a thinned-out version of the real chain (see section 2) implies that the scaling variables G^0_N and τ determine the subchain size q and the intrinsic friction coefficient γ. This is not immediately obvious because G^0_N and τ are expressed by Curtiss and Bird in terms of the parameters N, a, and ζ that characterize the model chain. However, the scaling picture requires that these parameters vary in proportion to those of the real chain, namely, N_u, a_u, and ζ_u. Thus the two unknowns, the scale factor q and the monomeric friction coefficient ζ_u, or equivalently q and γ, are determined by G^0_N and τ. Table I shows the original expressions obtained by Curtiss and Bird for G^0_N and τ, as well as the alternate version implied by scaling via eq 2.9–2.14. Additionally, any dependence on the molecular weight M has been made explicit by substituting

$$N = M/m = M/(qm_u) \tag{3.3}$$

where m_u is the monomer molecular weight, and

$$\nu = \rho N_{Avog}/M \tag{3.4}$$

where ν is the number density of polymer molecules in the melt of mass density ρ. In section 4 we use the CB model to obtain numerical values for q and γ in polystyrene melts.

We note that aside from its different theoretical approach, the model of Doi and Edwards[2] (DE) uses the same model chain and predicts nearly the same linear viscoelastic behavior as the CB model. Consequently, we can try to compare the values obtained for q and γ in each model. The reduced relaxation modulus $g_R(\tilde{t})$ in the DE model is in fact a special case of the CB result, obtained by setting the link tension coefficient ϵ equal to zero. Thus if the shape of the common reduced modulus can be fitted to a given set of experimental data with $\epsilon = 0$, the scale factors G^0_N and τ required for the adjustment will be the same for the CB and DE models. The difference between the numerical values for q and γ in the CB and DE models is due to the differing expressions for G^0_N and τ. Thus the DE formulas are also given in Table I, from which we see that the DE blob size will be four times that determined by the CB model:

$$q_{DE} = 4q_{CB} \tag{3.5}$$

Similarly, values of the frictional constant for the two models are related by

$$\gamma_{DE} = 2\gamma_{CB} \tag{3.6}$$

To obtain this result it is necessary to assume that the observed molecular weight dependence of the relaxation time τ is compatible with the fixed form specified by the DE model:

$$\tau \propto M^3 \tag{3.7}$$

This particular assumption would set $\beta = 0$ in the CB model. However, we remark that caution must be used when comparing the Doi–Edwards and Curtiss–Bird results via eq 3.5 and 3.6 since the physical meaning of q and γ is not precisely the same for each model.

Turning now to the shape of the modulus in the CB model, an equivalent description of the linear viscoelasticity is given by the complex modulus $G^*(\omega)$, obtained from $G(t)$ via the transform $i\omega\int_0^\infty dt\, e^{-i\omega t}G(t)$. In parallel with eq 3.2 then

$$G^*(\omega) = G^0_N g_R^*(\tilde{\omega}) \tag{3.8}$$

with the dimensionless frequency variable

$$\tilde{\omega} \equiv \omega\tau \tag{3.9}$$

The reduced complex modulus $g_R^*(\tilde{\omega})$ is discussed extensively in Appendix A, where closed-form expressions for it are derived, the limiting behavior at low frequencies is reviewed, and the asymptotic form at high frequencies is established.

We have computed the complete shape of the real and imaginary parts of g_R^*, shown by the dashed curves in Figures 1 and 2, respecively. Due to the presence of the link tension coefficient ϵ only in the imaginary part, the real part g_R' has a single universal curve (see Figure 1), while g_R'' has a sequence of curves varying with ϵ (see Figure 2). We note that this feature of the CB model is consistent with the Kramers–Kronig relation between the real and imaginary parts, because the ϵ-dependent term in g_R'' varies linearly with frequency and hence drops out of the Kramers–Kronig expression.

The dependence of the reduced loss modulus g_R'' on the link tension coefficient merits special attention in view of our earlier discussion in section 2 of the modified Stokes' law used in the CB model. There, we found the only value of ϵ consistent with the blob structure underlying the CB model chain is $\epsilon = 0$. To look at this result another way, nonzero values of ϵ imply an artificial rigidity of the model chain. This conclusion is striking because it demonstrates that the ϵ dependence of the dynamic viscosity $\eta'(\omega) = G^0_N g_R''(\tilde{\omega})/\omega$ in the CB model is consistent with the corresponding behavior observed in dilute solution theories when the rigidity of the chain structure is increased. In these theories one finds[15] that for bead–*spring* models the viscosity vanishes at high frequencies, while for bead–*rod* models the viscosity no longer vanishes. Additionally, it is found that when rigidity is increased in another way,

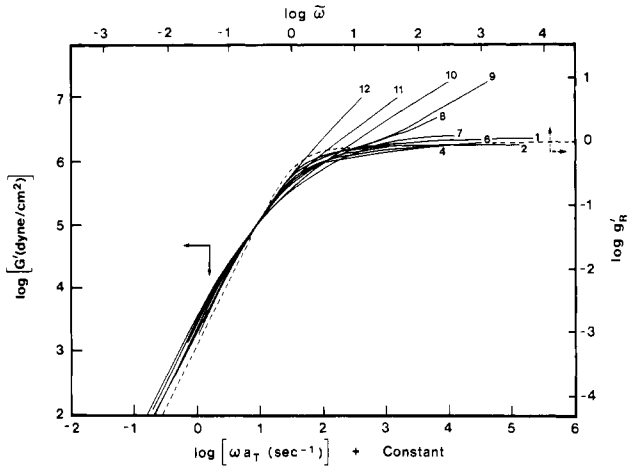

Figure 1. Comparison of the Curtiss–Bird model[1] with experiment for the storage moduli of narrow-distribution, linear, melt polystyrenes. Dashed curve: the reduced storage modulus $g_R'(\tilde{\omega}) \equiv G'(\omega)/G^0_N$ calculated from the CB model (see Appendix A), where G^0_N is the plateau storage modulus and $\tilde{\omega} \equiv \omega\tau$, τ being the characteristic relaxation time of the CB model. Solid curves: observed storage moduli $G'(\omega)$ for melt poystyrenes measured by Onogi et al.,[21] ranging in molecular weight from 12 000 to 616 000. The curve sequence (1, 2,..., 12) corresponds to the Onogi sample labels (L18, L19, L5, L22, L15, L27, L37, L16, L34, L14, L12, L9). The reference temperature was T = 160 °C. To focus on the shape of the modulus in the low-frequency terminal zone, the curves were shifted along the frequency axis until they coincided with the terminal zone of sample number 10.

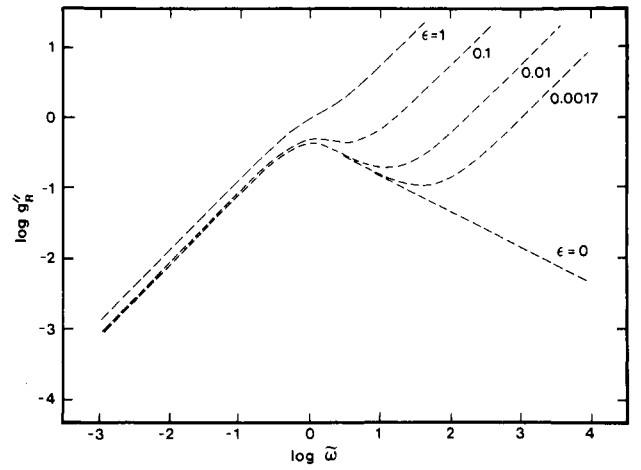

Figure 2. Theoretical form for the loss modulus $G''(\omega)$ as computed from the CB model (see Appendix A). The modulus is reduced to the universal form $g_R''(\tilde{\omega}) \equiv G''(\omega)/G^0_N$, where G^0_N is the plateau storage modulus and $\tilde{\omega} \equiv \omega\tau$, τ being the characteristic relaxation time of the CB model. The reduced loss modulus is plotted for values of the link tension coefficient ϵ between 0 and 1.

by replacing flexible chains by stiff chains, the viscosity is also increased at all frequencies. In the CB model, exactly similar behavior is observed for nonzero values of the link tension coefficient because ϵ makes a frequency-independent contribution $\epsilon(G^0_N\pi^2/18)$ to the dynamic viscosity (see eq A.25). Only when $\epsilon = 0$ does the dynamic viscosity have a limiting value $\eta'(\omega \to \infty)$ which is zero. Note that the CB form of η' must be compared with the intrinsic viscosity $[\eta']$ of dilute solution theories, because in the latter case the polymer molecules augment the Newtonian viscosity η_s, of the background solvent. We also hasten to point out that at high frequencies this comparison is only valid within the context of these models, because the range of validity of the models is limited to low and intermediate frequencies. The true reason for the

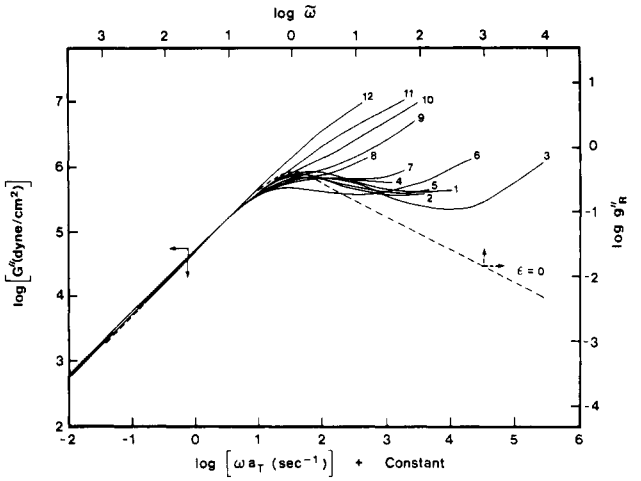

Figure 3. Comparison of experimental data with the predictions of the Curtiss–Bird model for the loss moduli $G''(\omega)$ of linear, narrow-distribution, melt polystyrenes. Dashed curve: the reduced loss modulus $g_R''(\tilde{\omega})$ in the CB model for the case of zero link tension coefficient (see Figure 2). Solid curves: loss moduli $G''(\omega)$ for the sequence of melt poystyrenes measured by Onogi et al.[21] (see caption to Figure 1).

observed nonzero high-frequency value of the intrinsic viscosity in dilute solutions remains obscure. It may indeed be related to the true bond constraints of real chains since rigidity inhibits the extremities of a molecule from adjusting to a velocity gradient and thereby enhances dissipation.[19] However, it may also result from excluded volume effects,[15] from hydrodynamic interaction effects,[15] or, we would add, from excitation of subchain modes.

In the next section we compare these inversal curves with dynamic measurements for polystyrene melts.

4. Comparison of the Curtiss–Bird Model with Melt Polystyrene Data

We compare the predictions of the CB model with the linear viscoelastic data obtained by Onogi et al.[21] for polystyrene melts. These authors measured detailed storage and loss modulus curves for a set of reasonably monodisperse polystyrene melts, covering a range of 12 000–616 000 in the weight-average molecular weight M_w. We first examine the degree to which the shape of the experimental curves is fitted by the theoretical reduced moduli g_R' and g_R'', using the fact that the nonreduced theoretical moduli G' and G'' have the same shape on a log G–log ω plot, shifted vertically and horizontally by log G^0_N and –log τ. Subsequently, the values of G^0_N and τ required to obtain the best alignment are used to determine the intrinsic properties of polystyrene chains relative to the CB model, namely, the subchain size q and the intrinsic friction coefficient γ (see section 3 and Table I).

To focus on the shape of the modulus curves, we have temporarily eliminated the experimental dependence of the characteristic relaxation time on molecular weight by horizontally shifting each log G–log ω curve until their terminal zones or low-frequency regions coincide. Since the slope of each curve in this region is slightly different, we have actually matched the curves at the frequency for which the log of the observed moduli is 5, an arbitrary choice. The unshifted curves are contained in the paper of Onogi et al. Our procedure is based on the fact that in view of the reptation picture, the CB model is intended to account for the microscopic processes that have the longest relaxation time scale and hence that determine the low-frequency end of the dynamic rheological behavior. Since these processes involve overall motions of the macromolecules, the time scale depends directly on molecular

weight. The universality of the theoretical curves occurs because there is a single time scale, τ.

Figures 1 and 3 contain the overlapping experimental storage and loss moduli G' and G'' as solid lines. The dashed lines are the moduli predicted by the CB model, with the loss modulus transferred from Figure 2 for the special case of zero link tension coefficient. These curves were obtained from the reduced moduli g_R' and g_R'', which were calculated from the expression for $G^*(\omega)$ provided by Curtiss and Bird (see Appendix A) and then shifted vertically and horizontally for alignment with the observed curves on account of the scale factors G^0_N and τ. For both storage and loss moduli, we found that the best alignment of the predicted and measured curves was produced by the same vertical and horizontal shift.

Aside from complications at the high-frequency end, the fit to the terminal zone as well as the conversion to a plateau in G' and a roll-off in G'' is reasonably described by the theoretical curves with $\epsilon = 0$. If the individual experimental curves are carefully distinguished it becomes evident that the knee separating the low-frequency zone from the intermediate frequency plateau region in G' and roll-off region in G'' softens as the molecular weight decreases. By contrast, the CB model predicts a knee that is always sharper. An initially broader knee might result from polydispersity, and an increasing breadth could be due to weakening of the reptational constraint for shorter chains or merging of the terminal and transition zones.

The transition zone refers to the high-frequency end of the moduli, where the moduli begin to increase again. Since this zone is independent of molecular weight, as shown in the unshifted curves of Onogi et al., it is associated with relaxational processes involving local motions of the macromolecules. In fact, our blob interpretation of the substructure of the CB model chain, introduced in section 2, implies that these motions involve the subchain structure neglected by the CB model. For the high molecular weight samples, the individual time scales of these two regions are well-separated, but as the molecular weight decreases, they eventually coalesce. It would be challenging to develop a unified model spanning the terminal and transition zones.

For the loss modulus curves in Figures 2 and 3, one might be tempted to select the theoretical curves with nonzero values of ϵ in order to match the local minima occurring in the data of Onogi et al. at frequencies above the knee. However, there are serious problems. That the minimum is in reality due to the presence of the transition zone constitutes the foremost objection. As just discussed, the CB model was only intended to describe the long-time rheology of melt systems, and it is more than likely that the transition zone must be understood by considering the internal structure of the submolecular blobs that comprise the reptating model chain. Overlooking this argument, other problems concern the conditions required to fit the minimum. Since the position and depth of the minimum in Figure 3 vary with molecular weight, following the plateau and eventually disappearing for smaller chains, it would be necessary to make ϵ dependent on the molecular weight. This serves merely to compensate the molecular weight dependence contained in the characteristic relaxation time of the CB model, because the theoretical loss curves of Figure 2 are in fact universal curves. It is not clear how a molecular weight dependence for ϵ could be justified in the CB model since ϵ appears to be a local property of the chain. Additionally, the data show no systematic dependence of the minimum on molecular weight, and if one attempts to fit the minimum at isolated molecular weights, the depth might be matched, or the width, but never both. One might instead try to fit the upper frequency transition zone, where the loss modulus again increases with frequency. Since the position of this zone is independent of M, in the absence of free volume effects, this can again only be attempted by having ϵ systematically increase with M. Also, the theoretical G'' must increase linearly with requency in this region according to the asymptotic behavior deduced in eq A.25. Actually, one finds the increase to be more gradual and to be accompanied by a similar increase in the storage modulus. The latter is not predicted at all by the theory, which indicates the plateau persists at arbitrarily high frequencies.

Turning now to the scale factors involved in fitting the Onogi data, from eq 3.8 the vertical shift required to fit the reduced moduli to the data is log G^0_N, and we find it to be 6.3 for both the storage and loss modulus curves. This corresponds to $G^0_N = 2 \times 10^6$ dyn cm^{-2} and enables us to determine the blob size in the model chain. From Table I this is given in the CB model by

$$q_{CB} = \rho RT/5m_u G^0_N \tag{4.1}$$

The polystyrene data were adjusted by Onogi et al. to a reference temperature of 160 °C. With $m_u = 104$ g/mol and $\rho = 1.05$ g cm^{-3} we then compute

$$q_{CB} \simeq 36 \text{ monomers/blob} \tag{4.2}$$

Given the subchain size q, the characteristic relaxation time τ determines the intrinsic friction coefficient γ (see section 3 and Table I), provided the molecular weight dependence is met. By eq 3.9, a direct method of determining τ for each molecular weight would be to measure the horizontal shift, $-\log \tau$, required to align the reduced theoretical curve with each experimental modulus curve. However, this procedure is subject to uncertainty owing to the lack of precise coincidence between the measured curves, as seen in Figures 1 and 3. We prefer to use the low-frequency behavior of the experimental curves in the terminal zone since in this region their limiting form is apparently well established.

The terminal zone at low frequencies is characterized for the loss modulus curve by the zero-shear rate viscosity η_0

$$\eta_0 = \lim_{\omega\to 0} G''(\omega)/\omega = G^0_N \tau \lim_{\tilde{\omega}\to 0} g_R''(\tilde{\omega})/\tilde{\omega} \tag{4.3}$$

and for the storage modulus curve by the elasticity coefficient A_G

$$A_G = \lim_{\omega\to 0} G'(\omega)/\omega^2 = G^0_N \tau^2 \lim_{\tilde{\omega}\to 0} g_R'(\tilde{\omega})/\tilde{\omega}^2 \tag{4.4}$$

The second version shown for each expression utilizes the reduced complex modulus defined in eq 3.8 and 3.9. In the CB model, eq A.22 and A.23 then give

$$\eta_0 = G^0_N \tau(\pi^2/12)[1 + (2/3)\epsilon] \tag{4.5}$$

and

$$A_G = G^0_N \tau^2 \pi^4/120 \tag{4.6}$$

Experimental values of η_0 and A_G were determined by Onogi et al. for their polystyrene melts using an unspecified extrapolation method and plotted against molecular weight. Reading from their curves,[21] we find

$$\log \eta_0 = 3.7 \log M_w - 12.3 \tag{4.7}$$

and

$$\log A_G = 7.5 \log M_w - 30.3 \tag{4.8}$$

where M_w is in g/mol. Since experimental measurements of dynamic moduli enable us to determine G^0_N, η_0, and A_G independently, both τ and ϵ can, in principle, be determined for each molecular weight using eq 4.5 and 4.6. Unfortunately, the experimental uncertainties are such that a negative value for ϵ would result, contrary to expectation in the model of Curtiss and Bird. As discussed in section 2, we also find on physical grounds that $\epsilon = 0$ seems to be the most plausible value for the link tension coefficient. Consequently, we set $\epsilon = 0$ and consider η_0 and A_G individually.

For the theoretical form of the zero-shear viscosity in eq 4.5 we substitute the expressions for G^0_N and τ listed in Table I. For the CB model

$$\eta_0 = (\rho N_{Avog}/120)M^{3+\beta}m_u^{-(2+\beta)}q^{-(2+\beta)}\gamma \quad (4.9)$$

where M and m_u are in g/mol. The experimental result of Onogi et al. in eq 4.7 is an example of the widely quoted[22] empirical relation

$$\eta_0 = KM^a \quad (4.10)$$

with $K = 10^{-12.3}$ and the zero-shear rate viscosity exponent $a = 3.7$. The molecular weight dependence is easily met in the CB model because the chain constraint exponent β entering eq 4.9 is unspecified. Thus if we compare eq 4.9 and 4.10 and set

$$\beta = a - 3 = 0.7 \quad (4.11)$$

then a combination of q and γ will be determined from viscosity data by

$$q^{-(2+\beta)}\gamma = K(\rho N_{Avog}/120)^{-1}m_u^{2+\beta} \quad (4.12)$$

With the above experimental values of K and β and the previously quoted values of m_u and ρ, this gives

$$q^{-2.7}\gamma = 2.66 \times 10^{-29} \quad (4.13)$$

Thus the intrinsic friction coefficient γ is determined by using eq 4.13 and the blob size $q \simeq 36$ determined above from the plateau modulus. Converting the units of m in $\gamma = \zeta a^2/m^2$ from g/mol back to g, we obtain

$$\gamma \simeq 1.57 \times 10^{23}\ \text{cm}^2/(\text{g-s}) \quad (4.14)$$

We can also determine γ from the elasticity data. Using eq 4.6 and Table I, the predicted form of the elasticity coefficient is

$$A_G = (\rho N_{Avog}/2400kT)M^{2(3+\beta)}m_u^{-(3+2\beta)}q^{-(3+2\beta)}\gamma^2 \quad (4.15)$$

When compared with the experimental result eq 4.8, this gives the analogue of eq 4.13

$$q^{-(3+2\beta)}\gamma^2 = 9.14 \times 10^{-56} \quad (4.16)$$

(We have adjusted the elasticity exponent in eq. 4.8 from 7.5 to 7.4 to maintain $\beta = 0.7$.) This yields

$$\gamma \simeq 2.97 \times 10^{23}\ \text{cm}^2/(\text{g-s}) \quad (4.17)$$

which is not identical with eq 4.14. The discrepancy corresponds to deviation between the theoretical and experimental value of the steady-state shear compliance $J^0_e \equiv A_G/\eta_0^2$.

We can also make an independent estimate of the intrinsic friction coefficient γ by recognizing that local properties of the chain should manifest themselves in the transition zone. We use our blob interpretation of the substructure of the model chain introduced in section 2, which implies that transition zone behavior is determined by chain motions at the subchain level. We also assume the subchain dynamics is described by the modified Rouse model of Ferry et al.[20] and is uncoupled from the reptational motions, which are frozen out at this shorter time scale. We assert that the applicable portion of the Rouse model is the intermediate frequency region in which the moduli are independent of *both* chain length and subchain size and obey

$$G'(\omega) = G''(\omega) = (\rho N_{Avog}/4)(\gamma kT\omega/3)^{1/2} \quad (4.18)$$

Since the slope of the empirical modulus curves of Onogi et al. is actually slightly steeper than $^1/_2$ in the transition zone region, we have estimated γ from eq 4.18 by inserting the values of ω at which the observed moduli are 10^7 dyn cm^{-2}. The result for the storage modulus is nearly identical with that for the loss modulus, and the average result is

$$\gamma_{Rouse} \simeq 2.21 \times 10^{25}\ \text{cm}^2/(\text{g-s}) \quad (4.19)$$

This is to be compared with the result given in eq 4.14, obtained by fitting the polystyrene data to the model of Curtiss and Bird in the terminal zone.

Another determination of γ in the modified Rouse model can be obtained[8] by using the Rouse expression

$$\eta_0(M)_{Rouse} = (\rho N_{Avog}\gamma/36)M \quad (4.20)$$

for the zero-shear viscosity in the nonentangled region $M < M_c$, where M_c is a critical molecular weight given by

$$M_c \simeq 10qm_u \quad (4.21)$$

Equation 4.21 follows from eq 4.1 and the relation $M_c \simeq 2\rho RT/G^0_N$ verified by Onogi et al.[21] Since eq 4.20 must agree with the CB model at the transition to entangled behavior, we equate eq 4.20 and 4.9 for $M = M_c$ and find

$$\gamma_{Rouse} = 3 \times 10^{1+\beta}\gamma_{CB} \quad (4.22)$$

Since γ_{CB} has the value given in eq 4.14 or 4.17, $\beta = 0.7$ gives

$$\gamma_{Rouse} = 2.36 \times 10^{25}\ \text{cm}^2/(\text{g-s}) \quad (4.23)$$

Table II summarizes the different values obtained for the intrinsic friction coefficient γ (at $T = 160$ °C) in melt polystyrene.

Table II
Two Different Determinations of the Intrinsic Friction Coefficient γ (See Eq 2.14) from Linear Viscoelastic Data of Onogi et al.[21] on Melt Polystyrene

γ, cm^2/(g·s)	method of determination	
10^{23}	zero-shear viscosity, elasticity coefficient	CB model
10^{25}	zero-shear viscosity ($M < M_c$), transition zone	modified Rouse model

5. Conclusion

Guided by dilute solution theory concepts and linear viscoelastic data on molten polystyrene, we have examined the physical basis of the recent model for polymer melt rheology proposed by Curtiss and Bird (CB).

We view the CB bead–rod model chain as a reduced or thinned-out version of the real chain, in which the rods are approximations to subchains of monomers, rather than single monomers. The objective of this or any scaling picture is to account for the dominant aspects of the molecular structure. The CB model accounts for chain flexibility and linear-chain geometry and incorporates reptational dynamics, but the constraint of fixed interbead separation implies a neglect of any effects resulting from internal degrees of freedom of the subchains. This contrasts with the bead–spring chain of the Rouse model.

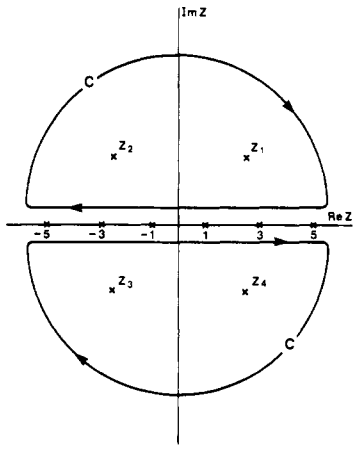

Figure 4. Evaluation of the reduced complex modulus $g_R^*(\tilde{\omega})$, using the contour integral in eq A.10 and A.16 to reduce infinite series expressions to closed form. We show the integration contour C and the location of simple poles in the integrand of eq A.10.

Thinking that effects of subchain structure might be contained in other aspects of the CB model, we considered the modified, CB form of Stokes' law, which is a statement about the interbead forces of constraint provided by the subchain structure. We found the only value of the link tension coefficient consistent with both internal subchain structure and the model chain bead–rod configuration is $\epsilon = 0$.

Comparing the CB model to linear viscoelastic data, we find that $\epsilon = 0$ gives a reasonable fit to the shape of the moduli in the terminal and plateau zones for narrow-distribution polystyrenes. Our scaling picture of the CB model chain rewrites the theoretical expressions for the plateau storage modulus G^0_N and the characteristic relaxation time τ in terms of the reduction factor or subchain size q and intrinsic properties of the real chain, For polystyrene, the experimental G^0_N and τ imply $q \simeq 36$ monomers per subchain and the intrinsic scalar Stokes' friction coefficient (at $T = 160$ °C) $\gamma \simeq 10^{23}$ cm^2/(g-s). The extraction of γ from the scaling picture is important because being an intrinsic chain property, it must enter other dynamical properties. In the transition zone, where only subchain dynamics should be manifested, we applied the modified Rouse model and found $\gamma \simeq 10^{25}$ cm^2/(g-s). Comparison of these independent determinations is interesting, but uncertainty in q affects the CB value of γ. Additionally, a unified model containing reptational and subchain dynamics is lacking.

The determination of the subchain size q contrasts with the Rouse model, where the applicable region of the theory is completely invariant to size of the subchains occurring in the reduced chain. The fact that the subchain size is determined by the CB model may be an artifact: in theories of rubber elasticity the plateau storage modulus is determined by the separation between cross-links; the CB model generates a similar expression for the plateau storage modulus but the quantity corresponding to the molecular weight between entanglements is $M_e = M_c/2 = 5qm_u$ (see eq 4.21). A problem with the CB model is that the role played by q remains uncertain, especially since constraint forces represented by entanglements appear to be absent from the stress tensor expression.

While the CB model presents difficulties in physical justification, it provides great potential for the study of polymer melt dynamics. Our study suggests several improvements for future extensions of the theory. Our main hope is that the simplifying scaling picture of the model chain be used and that interbead forces of constraint be eliminated in favor of a Rouse-like bead–spring model, with the extra condition of reptation. Additionally, the viscoelastic, non-Newtonian, many-body character of the background medium should be recognized if one hopes to fully understand corrections to the power law dependences predicted by the original version of the reptation model.

Acknowledgment. We thank Dr. W. M. Prest for a useful discussion of this problem and Mr. L. M. Marks for assistance with numerical computations and with derivation of the closed form of the theoretical moduli. D.A.B. thanks the Natural Sciences and Engineering Research Council of Canada for the award of an industrial postdoctoral fellowship.

Appendix A

Here we discuss the mathematical properties of the linear moduli in the CB model. We define the reduced modulus $g_R(\tilde{t})$ by factoring out the plateau modulus $G^0_N \equiv \nu NkT/5$ from the CB expression[1] for the relaxation modulus $G(t)$ (see eq 3.1 and 3.2) and by scaling time in terms of the characteristic relaxation time τ (see Table I). Thus

$$g_R(\tilde{t}) = (8/\pi^2) \sum_{n=1,3,...} (1/n^2) \exp(-\tilde{t}/\tilde{t}_n) + (\epsilon\pi^2/9)\delta(\tilde{t}) \tag{A.1}$$

where

$$\tilde{t} \equiv t/\tau \tag{A.2}$$

The spectrum $\{\tilde{t}_n\}$ of relaxation times, in units of τ, obeys

$$\tilde{t}_n = 1/n^2, \qquad n = 1, 3, ... \tag{A.3}$$

An equivalent representation of the linear viscoelasticity is given by the reduced complex modulus $g_R^*(\tilde{\omega})$, obtained from $g_R(\tilde{t})$ via the transform $i\omega\int_0^\infty dt\ e^{-i\omega t}$. This yields

$$g_R^*(\tilde{\omega}) = (8/\pi^2) \sum_{n=1,3,...} i\tilde{\omega}n^{-2}/[n^2(1 + i\tilde{\omega}n^{-2})] + (\epsilon\pi^2/18)i\tilde{\omega} \tag{A.4}$$

where the dimensionless frequency variable is

$$\tilde{\omega} \equiv \omega\tau \tag{A.5}$$

We derive a closed-form expression for $g_R^*(\tilde{\omega})$ by using contour integration. The real part of series in eq A.4 is

$$S'(\tilde{\omega}) = \sum_{n=1,3,...} \tilde{\omega}^2/[n^2(n^4 + \tilde{\omega}^2)] \tag{A.6}$$

and the imaginary part is

$$S''(\tilde{\omega}) = \sum_{n=1,3,...} \tilde{\omega}/[n^4 + \tilde{\omega}^2] \tag{A.7}$$

In other words, we have rewritten the reduced complex modulus as

$$g_R^*(\tilde{\omega}) = (8/\pi^2)[S'(\tilde{\omega}) + iS''(\tilde{\omega})] + (\epsilon\pi^2/18)i\tilde{\omega} \tag{A.8}$$

To evaluate the real part $S'(\tilde{\omega})$, we factor out $\tilde{\omega}^2$ and consider the series

$$S_1(\tilde{\omega}) \equiv S'(\tilde{\omega})/\tilde{\omega}^2 = \sum_{n=1,3,...} 1/[n^2(n^4 + \tilde{\omega}^2)] \tag{A.9}$$

We compute $S_1(\tilde{\omega})$ by using the contour integral

$$I_1(\tilde{\omega}) = \int_C \frac{\frac{1}{2}\pi \tan(\frac{1}{2}\pi z)}{z^2(z^4 + \tilde{\omega}^2)}\, dz \tag{A.10}$$

where the contour C is indicated in Figure 4. On the real axis, the integrand has a simple pole at $z = 0$ with residue $(^1/_2\pi)^2/\tilde{\omega}^2$, and the set of simple poles $\{...,-3,-1,1,3,...\}$, denoted by $\{x_k\}$, with the set of residues $\{-1/x_k^2(x_k^4 + \tilde{\omega}^2)\}$.

Consequently, the residue theorem implies

$$I_1(\tilde{\omega}) = 2\pi i[-2S_1(\tilde{\omega}) + (\tfrac{1}{2}\pi)^2/\tilde{\omega}^2] \quad (A.11)$$

The integral is also given in terms of the residues $\{^1/_2\pi \tan (^1/_2\pi z_k)/4z_k^5\}$ at the four off-axis simple poles

$$\{z_k\} = \{\tilde{\omega}^{1/2}e^{i\pi/4}, \tilde{\omega}^{1/2}e^{i3\pi/4}, \tilde{\omega}^{1/2}e^{-i3\pi/4}, \tilde{\omega}^{1/2}e^{-i\pi/4}\} \quad (A.12)$$

by the closed-form expression

$$I_1(\tilde{\omega}) = -2\pi i \sum_{k=1,2,3,4} \frac{\frac{1}{2}\pi \tan (\frac{1}{2}\pi z_k)}{4z_k^5} \quad (A.13)$$

Thus from eq A.11 and A.13 we find

$$S_1(\tilde{\omega}) = (\pi/16) \sum_{k=1,2,3,4} \frac{\tan (\frac{1}{2}\pi z_k)}{z_k^5} + \pi^2/8\tilde{\omega}^2 \quad (A.14)$$

Similarly, to obtain a closed-form expression for the imaginary part $S''(\tilde{\omega})$ of the series for g_R^*, we consider

$$S_2(\tilde{\omega}) \equiv S''(\tilde{\omega})/\tilde{\omega} = \sum_{n=1,3,\ldots} 1/(n^4 + \tilde{\omega}^2) \quad (A.15)$$

With the contour integral

$$\int_C \frac{\frac{1}{2}\pi \tan (\frac{1}{2}\pi z)}{z^4 + \tilde{\omega}^2} \, dz \quad (A.16)$$

we find

$$S_2(\tilde{\omega}) = (\pi/16) \sum_{k=1,2,3,4} \frac{\tan (\frac{1}{2}\pi z_k)}{z_k^3} \quad (A.17)$$

Using eq A.12, we find that eq A.14 and A.17 imply the low- and high-frequency behavior

$$S_1(\tilde{\omega} \to 0) \sim \pi^6/960 \quad (A.18)$$

$$S_2(\tilde{\omega} \to 0) \sim \pi^4/96 \quad (A.19)$$

and

$$S_1(\tilde{\omega} \to \infty) \sim \pi^2/8\tilde{\omega}^2 \quad (A.20)$$

$$S_2(\tilde{\omega} \to \infty) \sim (\pi/4(2^{1/2}))\tilde{\omega}^{-3/2} \quad (A.21)$$

Consequently, eq A.8, A.9, A.15, and A.18–A.21 imply that the real and imaginary parts of the reduced complex modulus have the limiting behavior

$$g_R'(\tilde{\omega} \to 0) \sim (\pi^4/120)\tilde{\omega}^2 \quad (A.22)$$

$$g_R''(\tilde{\omega} \to 0) \sim (\pi^2/12)[1 + (2/3)\epsilon]\tilde{\omega} \quad (A.23)$$

and the asymptotic property

$$g_R'(\tilde{\omega} \to \infty) \sim 1 \quad (A.24)$$

$$g_R''(\tilde{\omega} \to \infty) \sim (2^{1/2}/\pi)\tilde{\omega}^{-1/2} + (\epsilon\pi^2/18)\tilde{\omega} \quad (A.25)$$

To conclude this appendix, it is instructive to return to the time domain and consider the relaxation spectrum $H(t)$. It is related to the relaxation modulus by[22]

$$G(t') = \int_0^\infty H(t)t^{-1}e^{-t'/t} \, dt \quad (A.26)$$

Consequently, the reduced relaxation spectrum $h_R(\tilde{t}) \equiv H(\tilde{t}\tau)/G^0_N$ is

$$h_R(\tilde{t}) = (8/\pi^2) \sum_{n=1,3,\ldots} (1/n^4)\delta(\tilde{t} - n^{-2}) + (\epsilon\pi^2/18)\delta(\tilde{t}) \quad (A.27)$$

Thus the ϵ contribution can apparently be associated with a process having zero relaxation time. For times less than about 0.1τ, the spectrum contained in the sum is approximately a continuum, which we compute to be

$$h_R(\tilde{t})_{(\text{continuum})} \simeq (4/\pi)\tilde{t}^{1/2}, \qquad \tilde{t} < 0.1 \quad (A.28)$$

The increase in density of relaxational modes toward the high-frequency end is more than offset by their decreasing weight. This is responsible for the plateau in the storage modulus and the $\tilde{\omega}^{-1/2}$ decay in the loss modulus.

Registry No. Polystyrene, 9003-53-6.

References and Notes

(1) Curtiss, C. F.; Bird, R. B. *J. Chem. Phys.* **1981**, *74*, 2016, 2026.
(2) Doi, M.; Edwards, S. F. *J. Chem. Soc., Faraday Trans. 2* **1978**, *74*, 1789, 1802, 1818; **1979**, *75*, 38.
(3) de Gennes, P.-G. *J. Chem. Phys.* **1971**, *55*, 572.
(4) Edwards, S. F. *Proc. Phys. Soc.* **1967**, *92*, 9.
(5) de Gennes, P.-G. In "Scaling Concepts in Polymer Physics"; Cornell University Press: Ithaca, NY, 1979.
(6) Berry, G. C.; Fox, T. G. *Adv. Polym. Sci.* **1968**, *5*, 261.
(7) Klein, J. *Macromolecules* **1978**, *11*, 852.
(8) Graessley, W. W. *J. Polym. Sci., Polym. Phys. Ed.* **1980**, *18*, 27.
(9) Doi, M. *Polym. Prepr., Am. Chem. Soc., Div. Polym. Chem.* **1981**, *22*, 100.
(10) Wendel, H.; Noolandi, J. *Macromolecules* **1982**, *15*, 1318.
(11) Adam, M.; Delsanti, M., preprint.
(12) de Gennes, P.-G. Plenary Lecture, International Symposium on Macromolecules, Strasbourg, France, July 6–9, 1981.
(13) Bernard, D. A.; Noolandi, J. *Macromolecules* **1982**, *15*, 1553.
(14) Curtiss, C. F.; Bird, R. B.; Hassager, O. *Adv. Chem. Phys.* **1976**, *35*, 31.
(15) Bird, R. B.; Hassager, O.; Armstrong, R. C.; Curtiss, C. F. In "Dynamics of Polymeric Liquids"; Wiley: New York, 1977; Vol. 2.
(16) Rouse, P. E. *J. Chem. Phys.* **1953**, *21*, 1272.
(17) Ziman, J. M. In "Principles of the Theory of Solids", 2nd ed.; Cambridge University Press: London, England, 1972.
(18) Flory, P. J. *J. Chem. Phys.* **1949**, *17*, 303.
(19) Riseman, J.; Kirkwood, J. G. In "Rheology, Theory and Applications"; Eirich, F. R., Ed.; Academic Press: New York, 1956; Vol. 1.
(20) Ferry, J. D.; Landel, R. F.; Williams, M. L. *J. Appl. Phys.* **1955**, *26*, 359.
(21) Onogi, S.; Masuda, T.; Kitagawa, K. *Macromolecules* **1970**, *3*, 109.
(22) Graessley, W. W. *Adv. Polym. Sci.* **1974**, *16*, 1.